Geoderma 384 (2021) 114805

Contents lists available at ScienceDirect

Geoderma

journal homepage: www.elsevier.com/locate/geoderma

Reactive oxygen species alter chemical composition and adsorptive fractionation of soil-derived organic matter

Kaizad F. Patel [a,b,*], Václav Tejnecký [c,d], Tsutomu Ohno [a,*], Vanessa L. Bailey [b], Rachel L. Sleighter [c,d], Patrick G. Hatcher [c,d]

[a] School of Food and Agriculture, University of Maine, Orono, ME 04469-5722, USA
[b] Pacific Northwest National Laboratory, Biological Sciences Division, Richland, WA 99352, USA
[c] Department of Soil Science and Soil Protection, Faculty of Agrobiology, Food and Natural Resources, Czech University of Life Sciences Prague, Kamýcká 129, 165 00 Praha 6 – Suchdol, Czech Republic
[d] Department of Chemistry and Biochemistry, Old Dominion University, Norfolk, VA 23529, USA

ARTICLE INFO

Handling Editor: Ingrid Koegel-Knabner

Keywords:
Soil-derived organic matter
Adsorption
Goethite
Reactive oxygen species
Fenton reaction

ABSTRACT

Reactive oxygen species (ROS), formed during redox fluctuations in iron-rich soils, have been known to stimulate lignin degradation, although not much is known about how they alter soil organic matter (SOM) composition and interaction with mineral surfaces. We conducted a laboratory experiment to see how ROS altered SOM composition and adsorptive fractionation onto Fe-mineral surfaces. We reacted water extracts of SOM with ·OH, produced by the Fenton reaction, and then conducted a sorption experiment of the extracts with goethite to analyze the amount and quality of SOM adsorbed. The Fenton reaction preferentially consumed low-O, mostly aromatic molecules, and new high-O molecules were detected post-Fenton, nearly half of which were carbohydrate-like. Although the amount of C adsorbed did not change after oxidation, the post-Fenton adsorbed molecules were more oxidized. Pre-Fenton adsorption was dominated by aromatic molecules (90%), but post-Fenton, the adsorbed molecules were 75% aromatic and 25% carbohydrate-like. We show that the ·OH radical oxidized SOM and shifted patterns of adsorption to a more oxidized pool. Because adsorption to minerals is thought to stabilize SOM, our results suggest that ROS may alter the availability and stabilization patterns of SOM.

1. Introduction

The fate of soil organic carbon (SOC) depends on its potential biotic and abiotic interactions with soil components. Recent research has found that the water-soluble component of SOC adsorbed to metal (oxy) hydroxide surfaces has reduced bioavailability (Eusterhues et al., 2014; Mikutta et al., 2007; Schneider et al., 2010) and that the organic matter-mineral interaction is the dominant factor in the stabilization of SOC (Kleber and Johnson, 2010; Lehmann and Kleber, 2015; Schmidt et al., 2011). This finding has driven researchers to obtain a better understanding of the chemical process driving the interaction of dissolved organic matter (DOM) with mineral surfaces. The ultrahigh resolution capabilities of Fourier transform ion cyclotron resonance mass spectrometry (FT-ICR-MS) has shown in numerous studies that aromatic and aliphatic molecules with high O/C atomic ratios have high affinity for FeOOH and Al_2O_3 mineral surfaces (Avneri-Katz et al., 2017; Coward et al., 2018; Galindo and Del Nero, 2014; Lv et al., 2016). Studies that combined the use of atomic force microscopy (AFM) and FT-ICR-MS showed that higher molecular weight carboxyl-rich aromatic and N-containing aliphatic DOM molecules were correlated with high binding forces between DOM and iron (oxy)hydroxide functionalized AFM tips (Chassé and Ohno, 2016; Chassé et al., 2015). These studies clearly show that adsorptive fractionation of DOM is occurring on the mineral surfaces, with the enrichment of DOM components with higher affinity on the metal (oxy)hydroxide surface and those with lower affinity towards the mineral surfaces remaining in solution. The AFM studies provide strong support for the layer-by-layer "onion" model of DOM structuring, where carboxylic-rich aromatic and N-containing aliphatic molecules are initially involved in the DOM adsorption process (Coward et al., 2019; Kleber et al., 2007).

* Corresponding authors at: Pacific Northwest National Laboratory, Biological Sciences Division, Richland, WA 99352, USA (K.F. Patel). School of Food and Agriculture, University of Maine, Orono, ME 00469-5722, USA (T. Ohno).
E-mail addresses: kaizad.patel@pnnl.gov (K.F. Patel), ohno@maine.edu (T. Ohno).

https://doi.org/10.1016/j.geoderma.2020.114805
Received 1 July 2020; Received in revised form 9 October 2020; Accepted 21 October 2020

With adsorption to the mineral surface being a critical step in the stabilization process of soil C, soil processes that affect the chemical composition of SOC are likely to affect the persistence of soil C. FT-ICR-MS studies have consistently shown that lignin-like molecules make up the dominant fraction of soil DOM (Huang et al., 2019; O'Donnell et al., 2016; Ohno et al., 2014; Simon et al., 2018; Thieme et al., 2019). Further, lignin-derived organic matter has recently been shown to undergo aerobic abiotic oxidation by reactive oxygen species (ROS) through a series of reaction steps. The steps include: 1) the loss of methoxy groups, 2) the oxygenation of aromatic rings, 3) ring opening to form carboxylated olefins, 4) condensation to cyclic structures, and 5) radical-induced proton scavenging to form either carboxylated aromatics observed in soils or carboxylated alicyclic molecules (Heim and Schmidt, 2007; Klotzbücher et al., 2011, 2016; Waggoner et al., 2015; 2017). Recent work has also demonstrated the role of iron in the decomposition of lignin and soil organic matter (SOM). Hall & Silver (2013) demonstrated the production of ROS from the oxidation of Fe(II) in the tropical forest soils of Puerto Rico. These soils experience warm temperatures and frequent precipitation leading to repeated fluctuations in soil redox potential. They showed that fluctuating levels of soil O_2 drove soil Fe redox reactions, generating ROS that led to increased lignin biodegradation (Hall et al., 2016). A laboratory soil incubation study with Fe(II) addition showed that Fe(II) addition disproportionately reduced the mineralization of lignin, independent of O_2 availability (Hall et al., 2016). In addition, drier upland soils from diverse ecosystems also have high iron reduction potentials, which could affect iron-coupled processes such as lignin decomposition in non-tropical ecosystems (Yang and Liptzin, 2015).

The hydroxyl radical (·OH) is a powerful oxidant that can be generated in soils through the Fenton reaction (Petigara et al., 2002):

$H_2O_2 + Fe^{2+} \longrightarrow \cdot OH + OH^- + Fe^{3+}$.

In soils, the hydrogen peroxide (H_2O_2) can come from rainwater that averages 2–40 μmol L^{-1} H_2O_2 (Kok, 1980) or through in situ oxidation of Fe^{2+} and DOM by O_2 (Trusiak et al., 2018). Although there is some debate about the occurrence of the Fenton reaction outside of acidic pH (Miller et al., 2016), there is evidence of ·OH formation even at circumneutral pH in environmental systems (Grossman and Kahan, 2016; Petigara et al., 2002; Trusiak et al., 2018). The ·OH radical may also be formed by the oxidation of reduced SOM (Page et al., 2012). Climate-induced increases in both frequency and intensity of precipitation events (Prein et al., 2017) are likely to affect the frequency of soil redox cycling as soils undergo more rapid and intense wet-dry cycles. Understanding these dynamic soil processes will be increasingly important for understanding ecosystem services, such as the decomposition of SOM and stabilization of soil C associated with redox-active soil processes. The effects of ROS on lignin-derived DOM and aquatic DOM have been extensively investigated (Chen et al., 2014; Heim and Schmidt, 2007; Klotzbücher et al., 2011; Waggoner et al., 2017), however studies on ROS effects on soil-derived DOM have been limited.

The objective of this study was to investigate the effects of ·OH on the chemical composition and adsorptive behavior of soil-derived DOM. We hypothesized: (H1) lignin-like molecules would be consumed by the Fenton oxidation; (H2) post-Fenton extracts would show greater adsorption onto Fe-minerals, due to a greater proportion of oxidized SOM peaks; and (H3) the adsorbed fraction post-Fenton would be dominated less by lignin-like and more by oxidized aliphatic species. Two experiments were conducted to test these hypotheses: (i) addition of Fe^{2+} and H_2O_2 to SOM extracts to initiate the Fenton oxidation reaction and analysis of the resultant changes in SOM composition; and (ii) reaction of the native and Fenton-oxidized SOM extracts with goethite (FeOOH) and examination of differences in adsorptive fractionation. We used FT-ICR-MS to determine changes in the extracted SOM pool following the oxidation and adsorption treatments.

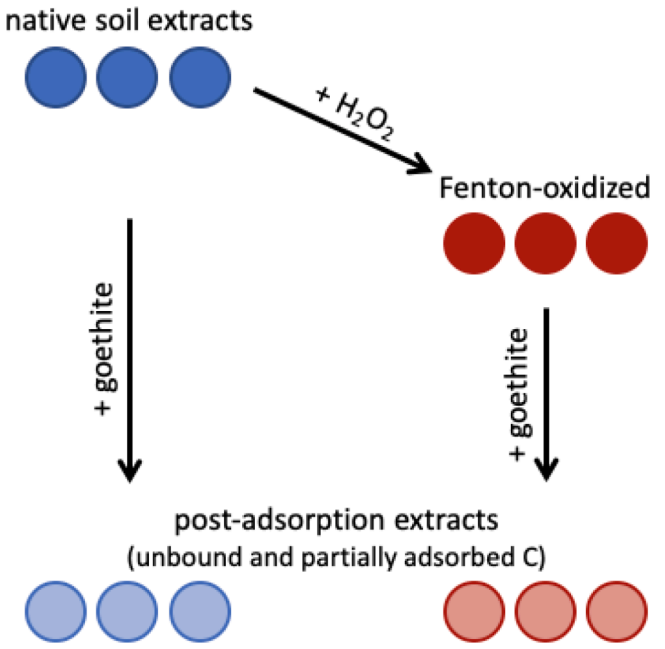

Fig. 1. Experimental setup. Organic C was extracted from soil with water, and half the extracts underwent the Fenton reaction with H_2O_2. Native and oxidized extracts were shaken with goethite to stimulate adsorption. The extracts were then filtered and prepared for analysis of the unbound/partially adsorbed DOM fraction. Extractions were performed in triplicate.

2. Experimental section

2.1. Dissolved organic matter and reaction with ·OH radical

Organic (Oe + Oi horizon) soils were collected from hardwood (HW) and softwood (SW) stands in the reference watershed of the Bear Brook Watershed in Maine (44°52'' N, 68°06′ W), U.S.A. These soils are classified as Typic Haplorthods, with organic horizons 5–10 cm thick with ~35–40% total carbon content (Patel et al., 2019). The two soils were extracted in triplicate with deionized distilled water (DI-H_2O) at a 1:10 w:v ratio for 16 h at 4 °C, centrifuged, and vacuum filtered through 0.4 μm Nuclepore polycarbonate filters.

A portion of each extract was retained to serve as the reference DOM prior to the oxidation and adsorption treatments. The DOM oxidation treatment used OH· radicals produced from the Fenton reaction (Waggoner et al., 2015). The DOM solution of ~300 ppm dissolved organic carbon (DOC) was adjusted to pH 3, and 4 mg $FeSO_4{\cdot}7H_2O$ was added to the solution, following the protocol of Waggoner et al. (2015). The ·OH formation was initiated by adding 2 mL of 30% H_2O_2 and was allowed to react for 1 h. The DOC concentration of the control and Fenton-oxidized extracts was measured using a Shimadzu TOC-V analyzer calibrated with potassium hydrogen phthalate.

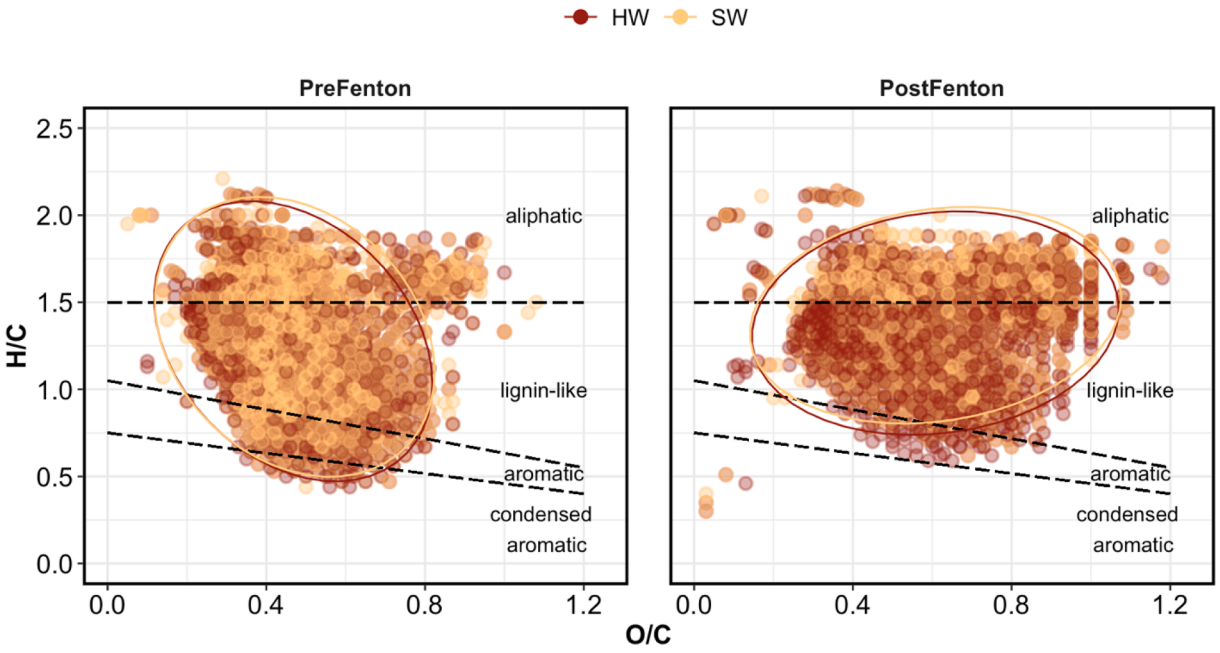

Fig. 2. Van Krevelen diagrams of molecular H/C and O/C ratios of DOM. Plots are for pre-Fenton (control) and post-Fenton DOM molecules in hardwood (HW) and softwood (SW) soils. Of the 1860 unique peaks in the pre-Fenton extracts, 1416 were common to both forest types. Of the 1784 unique peaks detected in the post-Fenton extracts, 1276 were common to both forest types. Density ellipses represent the 95% confidence regions.

2.2. Adsorption experiments

Batch DOM adsorption studies were conducted on goethite with the untreated control extracts (pH 3.05 in HW – 4.07 in SW) and the Fenton-oxidized extracts (Fig. 1). We must note that not all iron minerals exhibit the same sorptive behavior, and that other minerals such as ferrihydrite have been found to show stronger adsorptive fractionation of SOM (Lv et al., 2016). Goethite was chosen because it is the most stable Fe mineral in forest soils (Cornell et al., 2007). Catalysis-grade goethite (FeOOH) (Sigma-Aldrich #371254) was used after repeated rinsing with DI-H_2O. A suspension of 1.00 g FeOOH in 30 mL of DOM solution (starting at ~300 ppm DOC) was shaken in glass Erlenmeyer flasks on an orbital shaker for 48 h at 4 °C. Controls were established with DI-H_2O plus FeOOH. The solutions were then filtered and analyzed for their DOC concentrations as described above. The quantity adsorbed was calculated by difference from the initial DOC solution concentration.

2.3. ESI-FT-ICR-MS analysis

The extracts were processed through Agilent PPL solid-phase extraction cartridges to desalt the extract for subsequent electrospray ionization (ESI) FT-ICR-MS analysis (Dittmar et al., 2008). The DOM was characterized in triplicate using negative ion mode ESI with a 12 T Bruker Daltonics Apex Qe FT-ICR-MS instrument at the College of Sciences Major Instrumentation Cluster (COSMIC) facility at Old Dominion University. To increase the ionization efficiency, ammonium hydroxide was added immediately prior to ESI to raise the pH to 8. Samples were introduced by a syringe pump at an infusion rate of 120 μL h^{-1} and analyzed in negative ion mode with electrospray voltages optimized for each sample. Ions (in the range of 200–2000 *m/z*) were accumulated in a hexapole for 1.0 sec before being transferred to the ICR cell. Exactly 300 transients, collected with a 4 MWord time domain, were added for a total run time of ~30 min. The summed free induction decay signal was zero-filled once and Sine-Bell apodized prior to fast Fourier transformation and magnitude calculation using the Bruker Daltonics Data Analysis software. Prior to data analysis, all samples were externally calibrated with a polyethylene glycol standard and internally calibrated with naturally present fatty acids within the sample (Sleighter et al., 2008).

2.4. Mass spectra data post-processing

For assignments of molecular formulas, peaks with a signal to noise ratio above 5 were assigned using the Formularity program developed by the Pacific Northwest National Laboratory (Tolić et al., 2017; Kujawinski and Behn, 2006). The FT-ICR-MS spectra are presented in Appendix A1. The assigned formulas were parsed into the appropriate van Krevelen space, which consisted of six discrete regions based on molecular H/C and O/C ratios, and the modified aromaticity index, AI_{mod} (Seidel et al., 2014; Koch and Dittmar, 2016): (1) condensed aromatic molecules ($AI_{mod} > 0.66$); (2) aromatic molecules ($0.66 \geq AI_{mod} > 0.50$); (3) highly unsaturated lignin-like molecules ($AI_{mod} \leq 0.50$ and $H/C < 1.5$); (4) carbohydrate-like molecules ($H/C \geq 1.5$ and $O/C \geq 0.6$); (5)

Table 1
Relative abundance (percentage) of groups in hardwood and softwood SOM, for initial (pre-Fenton) and post-Fenton extracts. Asterisks represent significant differences between pre- and post-Fenton extracts for a given forest type ($\alpha = 0.05$).

	Hardwood		Softwood	
	PreFenton	PostFenton	PreFenton	PostFenton
DOC concentration, mg/L	497 ± 40	458 ± 34	515 ± 6	455 ± 7*
No. of assigned formulas	1562	1675	1714	1385
Class %				
Condensed Aromatic	2.5	0.3	1.9	0.3
Aromatic	10.1	3.5	8.9	1.7
Lignin-like	54.8	56.0	53.6	51.6
Carbohydrate-like	7.3	24.0	8.6	27.4
Aliphatic-noN	14.9	9.7	18.2	14.3
Aliphatic + N	10.4	6.5	8.8	4.7

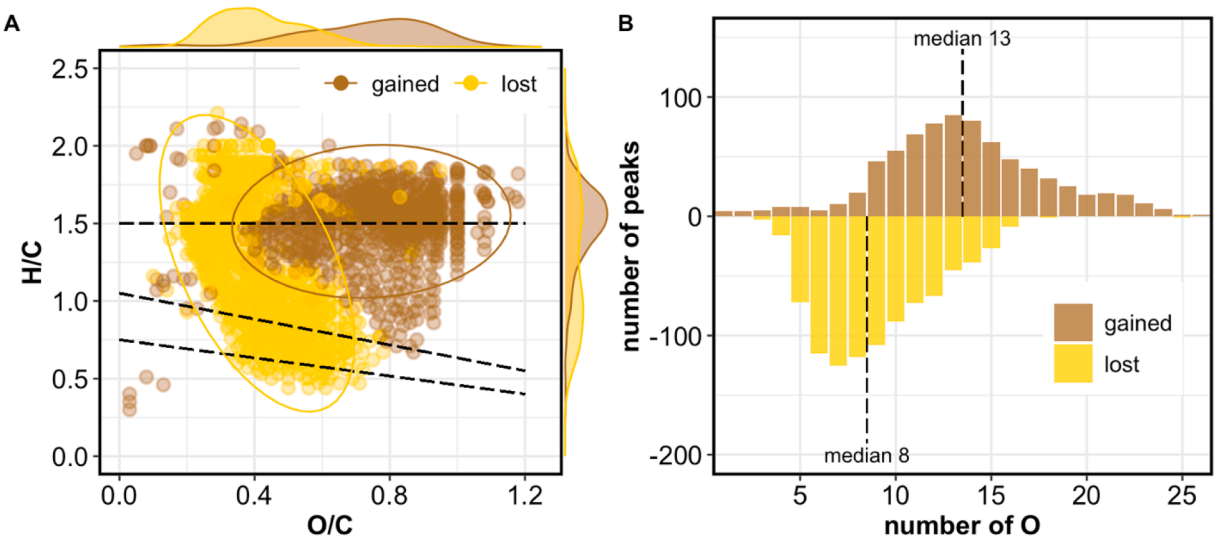

Fig. 3. (A) Van Krevelen diagrams of molecules gained or lost following oxidation via the Fenton reaction, combined for hardwood and softwood soils. The ellipses represent the 95% confidence region for the respective treatments. Marginal plots show the density distribution of peaks along the two axes. (B) Molecules lost and newly formed following the Fenton oxidation, binned by the number of oxygen atoms. Negative values on the y-axis represent the peaks lost.

Table 2
Number of peaks lost, gained, and conserved following the Fenton oxidation, calculated for hardwood and softwood soils.

Class	lost	gained	conserved
Condensed aromatic	41	5	1
Aromatic	148	4	57
Lignin-like	405	316	680
Carbohydrate-like	21	347	141
Aliphatic-noN	171	49	175
Aliphatic + N	121	37	79
Total	907	758	1133

non-N containing aliphatic molecules (H/C $\geq$ 1.5, O/C $<$ 0.6, N $=$ 0); and (6) N containing aliphatic molecules (H/C $\geq$ 1.5, O/C $<$ 0.6, N $\geq$ 1). We caution that these compound categories are tentative classifications, because they are based on H/C, O/C, and AI_{mod} indices, and not the actual molecular structure. We therefore refer to these classes as "carbohydrate-like" and "lignin-like" and not simply "carbohydrate" and "lignin".

Further post-processing of FT-ICR-MS data was performed using the *fticrrr* workflow in R (Patel, 2020). To avoid biases of ESI (see Ohno et al., 2016), we report all FT-ICR-MS data in terms of peak counts and not intensities. Peaks were determined using a presence/absence

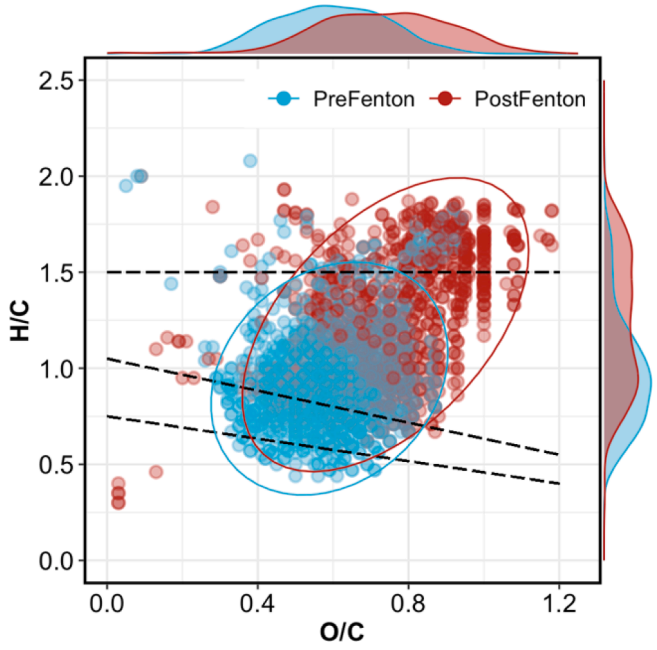

Fig. 4. Van Krevelen plot showing goethite-adsorbed peaks for pre- and post-Fenton extracts, combined for hardwood and softwood soils. Marginal plots show the density distribution of peaks along the two axes. Adsorbed peaks had a median O/C of 0.61 for pre-Fenton and 0.75 for post-Fenton extracts.

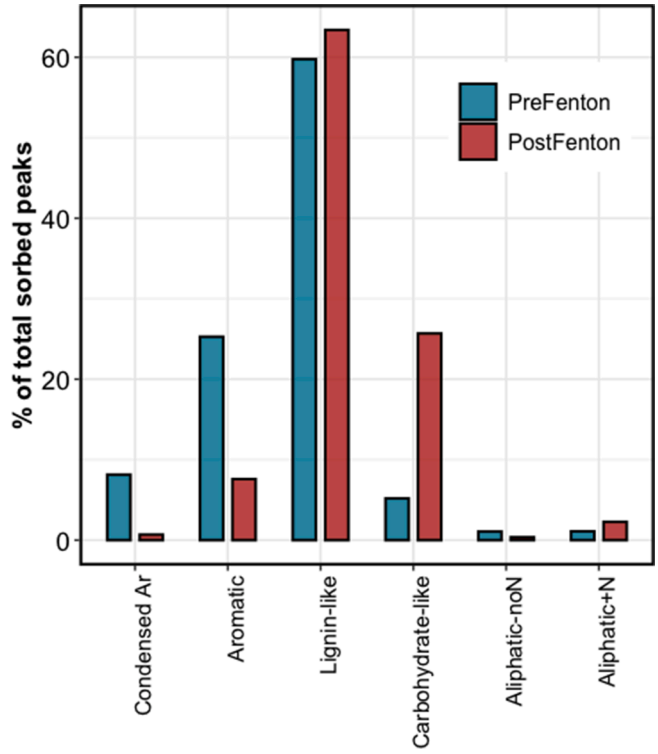

Fig. 5. Contribution of organic classes to the goethite-adsorbed fraction, for pre- and post-Fenton extracts, combined for hardwood and softwood soils.

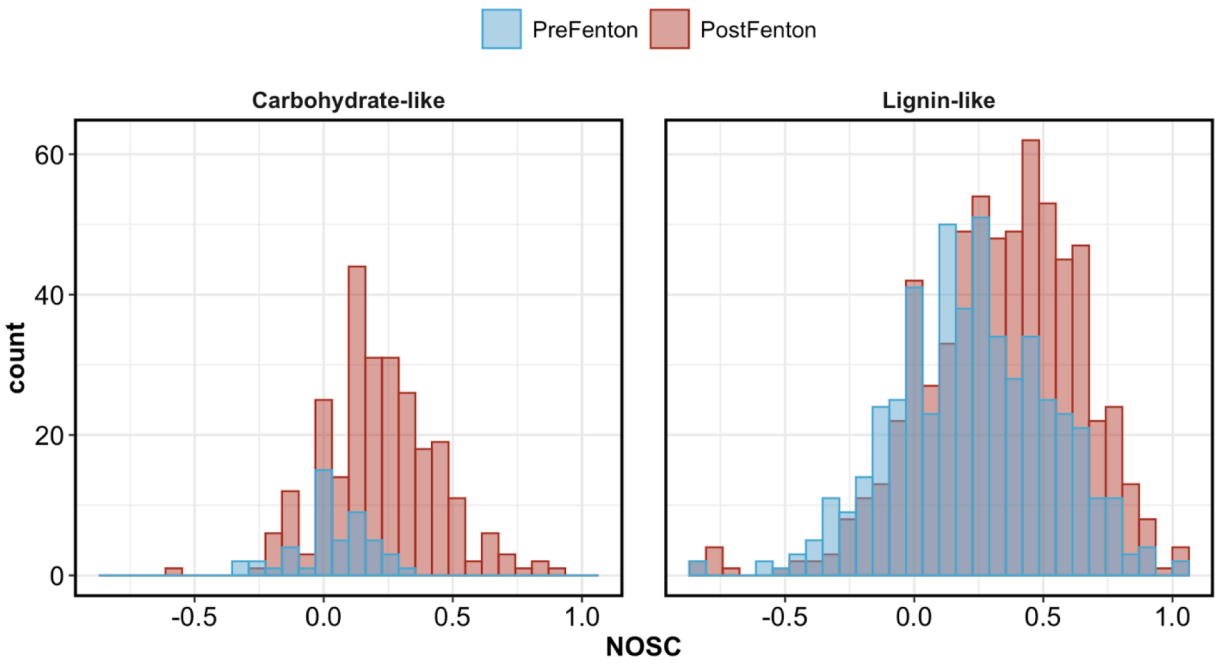

Fig. 6. Frequency distribution of adsorbed peaks, by the nominal oxidation state of carbon (NOSC) for pre-Fenton and post-Fenton extracts, combined for hardwood and softwood soils. Only carbohydrate-like and lignin-like peaks are reported here. The post-Fenton adsorbed pool was shifted to a more oxidized state.

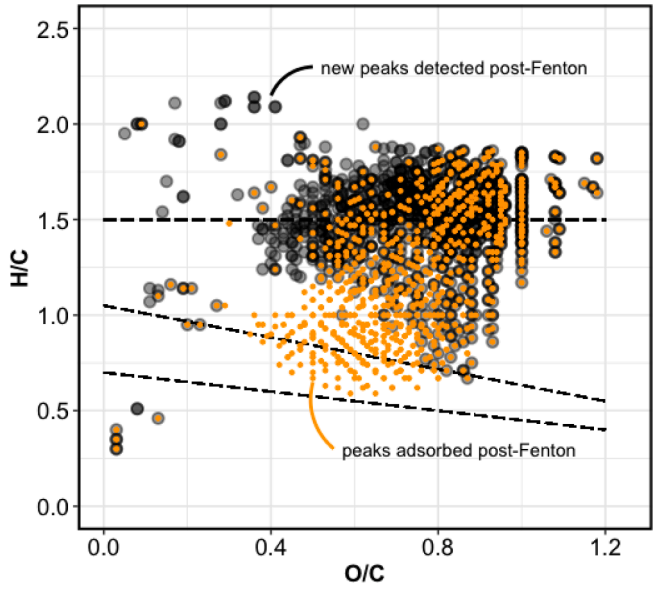

Fig. 7. Van Krevelen plot for post-Fenton extracts (HW and SW combined), showing the newly detected peaks after Fenton oxidation (black) and all the adsorbed peaks (orange). Nearly 60% of the newly detected peaks were adsorbed onto goethite. (For interpretation of the references to colour in this figure legend, the reader is referred to the web version of this article.)

technique, including only peaks present in all three experimental replicates. Relative abundances of the different molecular groups were calculated using peak counts, as the ratio of counts per molecular group to the total counts per sample. Nominal oxidation state of carbon (NOSC) was derived from molecular formulas using the following formulas from Riedel et al. (2012):

$$NOSC = 4 - [(4c + h - 3n - 2o - 2s)/c]$$

where c, h, n, o, and s refer to the stoichiometric numbers of carbon, hydrogen, nitrogen, oxygen, and sulfur atoms per formula, respectively.

Adsorptive fraction was determined by comparing pre- and post-goethite extracts. Molecules present in the pre-goethite extracts but not in the post-goethite extracts were completely adsorbed, hereafter called "sorbed". Molecules that were present in both pre- and post-goethite extracts were theoretically either completely unbound (not adsorbed) or partially adsorbed.

3. Results and discussion

The van Krevelen diagrams in Fig. 2 show the distribution of molecules in the native and post-Fenton SOM-derived pools as defined by their H/C and O/C ratios. In general, SOM composition did not differ between forest types for pre- or post-Fenton extracts, with ~76% of the total peaks shared by both hardwood and softwood soils. The native (pre-Fenton) soil extracts were dominated by lignin-like molecules (~50–55%), and aliphatic peaks (with and without N, and carbohydrate-like) made up ~30–35% of total peaks identified (Table 1).

3.1. Oxidation altered DOC concentration and composition

The OH radical generated by the Fenton reaction has been linked to lignin degradation (Hall et al., 2015), and we expected that lignin-like peaks would be consumed by the Fenton reaction, i.e. fewer lignin-like peaks being assigned in post-Fenton solutions (hypothesis H1). However, the relative abundance of lignin-like molecules remained fairly constant (Table 1), although this fraction was more oxidized post-Fenton (Fig. 2). Low-oxygen lignin-like peaks were lost, and new peaks were detected with higher O content (Fig. 3a), partially confirming H1 and similar to findings for lignin oxidized by the Fenton reaction (Waggoner et al., 2015, 2017).

Following the Fenton reaction, there was a significant decline in the DOC concentrations (Table 1), as well as a change in the SOM molecular composition (Fig. 2, Table 1), suggesting partial oxidation of the DOM components. Of the 907 peaks lost in the Fenton reaction, ~65% were aromatic, condensed aromatic, and lignin-like (Table 2). Post-Fenton extracts showed a 3-fold increase in detected carbohydrate-like peaks (Table 1).

As expected, the Fenton oxidation shifted the DOM to a more

oxidized pool, as the ·OH radical reaction preferentially consumed DOM molecules with ≤ 8O atoms and the newly detected molecules had ≥ 13O atoms (median values, Fig. 3b). There was a concurrent increase in the nominal oxidation state of carbon (NOSC) for the DOM pool, with a median NOSC of +0.2 post-Fenton, compared to −0.2 pre-Fenton. Since oxygen content has been linked to adsorption capacity (Young et al., 2018; Ohno et al., 2018; Lv et al., 2016), it is expected that this increased oxidation would increase the amount of adsorbed carbon when reacted with goethite.

3.2. Oxidation altered goethite adsorption patterns of DOM

Approximately 70–80% of the extracted DOC was adsorbed onto goethite (10.6 ± 0.3 mg C g^{-1} goethite). Contrary to our expectations (hypothesis H2), the amount of adsorbed C remained unchanged by the Fenton reaction. There was, however, a shift in the types of molecules sorbed, as more oxidized molecules were adsorbed post-Fenton, confirming hypothesis H3 (Figs. 4, 5).

In the pre-Fenton extracts, approximately 90% of the goethite-sorbed peaks were condensed aromatic, aromatic, and lignin-like molecules; in post-Fenton extracts, the contribution of aromatic and condensed aromatic peaks was reduced, only 75% of goethite-sorbed peaks, driven by the disappearance of those peaks after Fenton oxidation. Instead, carbohydrate-like molecules contributed ~25% to the goethite-sorbed peaks, a 5-fold increase from the pre-Fenton extracts (Fig. 5). Lignin-like peaks accounted for ~60% of total adsorbed peaks, for both pre- and post-Fenton extracts (Fig. 5), although the goethite-sorbed molecules were more oxidized post-Fenton (Fig. 6). The high adsorption of lignin is not surprising, because the high prevalence of carboxyl groups promotes ligand exchange reactions with Fe mineral surfaces, especially at the low pH of these samples (Guggenberger et al., 1998; Coward et al., 2018; Dai et al., 1996). Outer-sphere hydrophobic interactions may also promote adsorption of the DOM to the goethite (Kleber et al., 2015). It is noteworthy that the adsorbed lignin molecules were more oxidized post-Fenton (Fig. 6), consistent with changes in the overall DOM pool (Fig. 3a).

The shift in adsorptive patterns described here can have strong implications for SOM availability, since organo-mineral interactions help stabilize SOM molecules. Mineral adsorption typically favors aromatic compounds, which make up the primary adsorption layer of the multilayer onion model (Coward et al., 2018; Ohno et al., 2018). Lv et al. (2016) demonstrated that goethite showed less adsorptive fractionation than other Fe-minerals like ferrihydrite, but it still preferentially adsorbed aromatic and high-O molecules. Young et al. (2018) demonstrated with Fe-montmorillonite that non-selective adsorption of DOM exceeded selective adsorption and that the adsorption patterns reflected the initial character of the solutions. We see similar results, as the fraction of goethite-sorbed molecules shifted to a more oxidized character after the Fenton oxidation reaction. Of the 758 new peaks observed after Fenton oxidation, nearly 60% were adsorbed onto goethite (Fig. 7).

Although not studied in this experiment, the presence of more oxidized molecules, such as those detected following the Fenton reaction, would likely also shift the DOM pool to a more labile state, since (a) these peaks have been found to be strongly correlated with biodegradability (Ohno et al., 2014); and (b) greater NOSC values suggest greater thermodynamic favorability for microbial metabolism (Graham et al., 2017; LaRowe and Van Cappellen, 2011). However, these oxidized molecules were also adsorbed onto the goethite, suggesting that these more biodegradable molecules may actually remain unavailable for microbial consumption in the presence of high clay concentrations.

The FT-ICR-MS analysis provides ultrahigh resolution data that enable SOM characterization and offer insights into the origins of the SOM, but its limitations, such as preferential ionization of lignins and aromatics, and suppression of carbohydrates (Ohno et al., 2016), highlight that it is not ideal for quantitative analysis. In addition to FT-ICR-MS, we performed ^{13}C nuclear magnetic resonance (NMR) spectroscopy on the pre- and post-Fenton soil extracts, for a more quantitative characterization of the SOM (see Appendix A2). The ^{13}C NMR indicated that o-alkyl groups, which are typical of carbohydrates, alcohols, and ethers, accounted for approximately half of the identified peaks (Appendix Table A2). Although the carbohydrate (o-alkyl) content remained relatively unchanged post-Fenton, the increase in carboxyl C content suggests an oxidation of the carbohydrate groups. The Fenton reaction is known to target lignin- as well as carbohydrate-like molecules (Moody, 1963; Morelli et al., 2003; Waggoner et al., 2017), and our results are consistent with this. There thus seems to be an increase in the ionizable carbohydrate content post-Fenton, which would result in improved detection of carbohydrate-like peaks with FT-ICR-MS as well as increased adsorption of these peaks to goethite, as discussed earlier in the manuscript. These results demonstrate the utility of a more comprehensive approach for SOM characterization, building on the complementary strengths of analyses such as FT-ICR-MS and NMR.

4. Conclusions

This study demonstrates how oxidation by ·OH alters the adsorptive fractionation of DOM onto goethite, as high O-containing lignin-like and carbohydrate-like molecules are adsorbed onto the Fe mineral surfaces. Reactive oxygen species are generated during redox fluctuations in Fe-containing soils (Trusiak et al., 2018), and as the water cycle intensifies, the fluctuating soil moisture conditions will likely result in increased ROS generation. Understanding these changing organo-mineral interactions becomes increasingly critical in a changing environment, since they can have implications for carbon availability in soils.

Data availability

Data are archived at the Environmental Data Initiative (package ID edi.634.1, https://portal.edirepository.org/nis/mapbrowse?packageid=edi.634.1). R scripts for data processing, analysis, and visualization are available at https://github.com/kaizadp/fenton_adsorption_SOM. (https://doi.org/10.5281/zenodo.420245).

Declaration of Competing Interest

The authors declare that they have no known competing financial interests or personal relationships that could have appeared to influence the work reported in this paper.

Acknowledgments

This project was supported by USDA-NIFA-2018-67019-27801, the Maine Agricultural and Forest Experiment Station (MAFES) Hatch Project ME-02163, and the U.S. Department of Energy, Office of Science, Biological and Environmental Research as part of the Terrestrial Ecosystem Sciences Program. Soil samples were collected from the Bear Brook Watershed in Maine, a site funded by the National Science Foundation (DEB-1119709).

Appendix A1. FT-ICR-MS spectra

Fig. A1

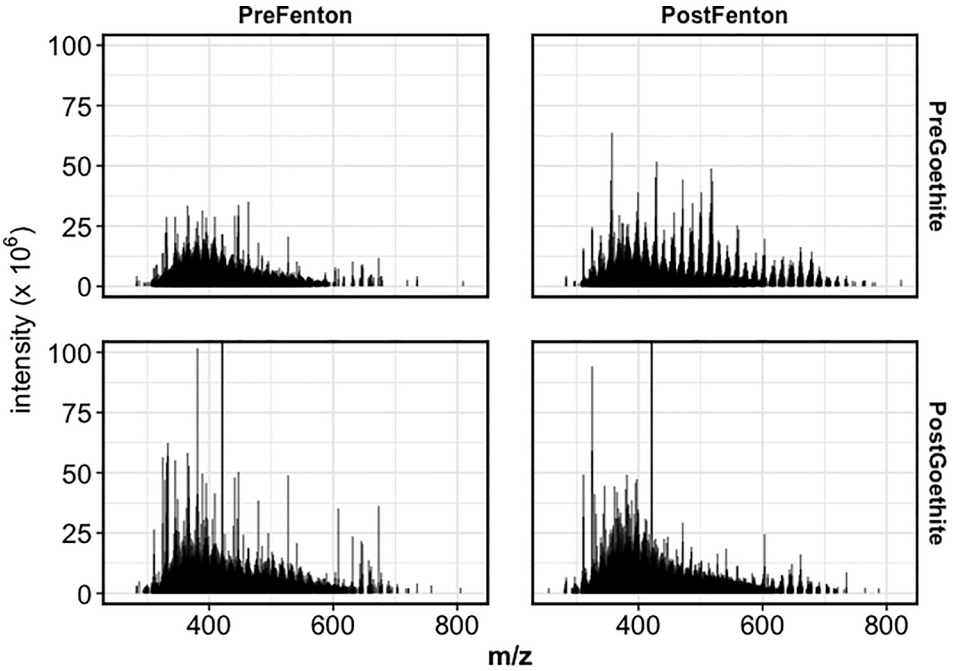

Fig. A1. FT-ICR-MS spectra for pre- and post-Fenton extracts, before and after reaction with goethite. The adsorbed fraction was determined by subtracting the post-Goethite from the pre-Goethite spectra.

Table A1
Relative abundance (percentage) of groups in pre- and post-Fenton extracts.

Functional group (ppm shift)	Hardwood		Softwood	
	Pre-Fenton	Post-Fenton	Pre-Fenton	Post-Fenton
carbonyl C (190–220)	1.0	1.0	1.1	1.2
carboxyl C (165–190)	12.4	15.0	9.3	10.7
aromatic C (112–165)	6.1	5.3	5.0	3.4
anomeric C (90–112)	11.6	13.6	12.9	14.2
O-alkyl C (58–90)	51.2	46.3	57.7	51.8
methoxy C (54–58)	2.9	4.0	2.3	2.8
aliphatic C (5–54)	14.9	14.8	11.6	15.9
Total	100	100	100	100

Appendix A2. Solid-state ^{13}C NMR data for pre- and post-Fenton samples

^{13}C nuclear magnetic resonance (NMR) spectroscopy was performed on a limited number of samples (n = 1) to quantify the relative proportions of functional groups in the DOC extracts.

Soil extracts were frozen and then freeze-dried. Solid-state ^{13}C NMR experiments were performed by a double resonance technique on a Bruker Advance II spectrometer with ^{1}H resonating at 400 MHz and ^{13}C resonating at 100 MHz. The NMR was equipped with a 4 mm H-X magic angle spinning probe head. The ^{13}C chemical shifts were calibrated to a glycine external standard (176.03 ppm). Quantitative ^{13}C NMR spectra with a multi-CP (cross polarization) pulse program have been shown to be comparable to direct polarization NMR experiments but with greater signal-to-noise ratios (Johnson and Schmidt-Rohr, 2014). Samples of approximately 80 mg were packed into zirconium rotors and sealed with Kel-F caps for analysis. Acquisition parameters were optimized per sample using the multi-CP approach, acquiring 5008 scans and a magic-angle spinning rate of 14 kHz. The spectra were integrated into seven regions (Table A1), calculated as the sum of peak areas within the region. We report the relative abundance of each region calculated as the proportion of signal in each region to the total across all regions, normalized to 100%.

^{13}C NMR data showed that the o-alkyl groups (typical of carbohydrates, alcohols, and ethers) accounted for approximately half of all detected groups. Relative contributions of the functional groups did not differ significantly by forest type (hardwood vs. softwood) or even by the Fenton oxidation reaction (pre-Fenton vs. post-Fenton).

References

Avneri-Katz, Shani, Young, Robert B., McKenna, Amy M., Chen, Huan, Corilo, Yuri E., Polubesova, Tamara, Borch, Thomas, Chefetz, Benny, 2017. Adsorptive fractionation of dissolved organic matter (DOM) by mineral soil: Macroscale approach and molecular insight. Org. Geochem. 103, 113–124.

Chassé, Alexander W., Ohno, Tsutomu, 2016. Higher molecular mass organic matter molecules compete with orthophosphate for adsorption to iron (oxy)hydroxide. Environ. Sci. Technol. 50 (14), 7461–7469.

Chassé, Alexander W., Ohno, Tsutomu, Higgins, Steven R., Amirbahman, Aria, Yildirim, Nadir, Parr, Thomas B., 2015. Chemical force spectroscopy evidence supporting the layer-by-layer model of organic matter binding to iron (oxy) hydroxide mineral surfaces. Environ. Sci. Technol. 49 (16), 9733–9741.

Chen, H., Abdulla, H.A.N., Sanders, R.L., Myneni, S.C.B., Mopper, K., Hatcher, P.G., 2014. Production of black carbon-like and aliphatic molecules from terrestrial dissolved organic matter in the presence of sunlight and iron. Environ. Sci. Technol. Lett. 1 (10), 399–404. https://doi.org/10.1021/ez5002598.

Cornell, Rochelle M., Schwertmann, U., 2007. The Iron Oxides: Structure, Properties, Reactions, Occurrences and Uses. John Wiley & Sons, Weinheim.

Coward, Elizabeth K., Ohno, Tsutomu, Plante, Alain F., 2018. Adsorption and molecular fractionation of dissolved organic matter on iron-bearing mineral matrices of varying crystallinity. Environ. Sci. Technol. 52 (3), 1036–1044.

Coward, Elizabeth K., Ohno, Tsutomu, Sparks, Donald L., 2019. Direct evidence for temporal molecular fractionation of dissolved organic matter at the iron oxyhydroxide interface. Environ. Sci. Technol. 53 (2), 642–650.

Dai, K'o H., David, Mark B., Vance, George F., 1996. Characterization of solid and dissolved carbon in a spruce-fir spodosol. Biogeochemistry 35 (2), 339–365.

Dittmar, Thorsten, Koch, Boris, Hertkorn, Norbert, Kattner, Gerhard, 2008. A simple and efficient method for the solid-phase extraction of dissolved organic matter (SPE-DOM) from seawater. Limnol. Oceanogr-Meth. 6 (6), 230–235. https://doi.org/10.4319/lom.2008.6.230.

Eusterhues, Karin, Neidhardt, Julia, Hädrich, Anke, Küsel, Kirsten, Totsche, Kai Uwe, 2014. Biodegradation of ferrihydrite-associated organic matter. Biogeochemistry 119 (1–3), 45–50.
Galindo, Catherine, Del Nero, Mirella, 2014. Molecular level description of the sorptive fractionation of a fulvic acid on aluminum oxide using electrospray ionization fourier transform mass spectrometry. Environ. Sci. Technol. 48 (13), 7401–7408.
Graham, Emily B., Tfaily, Malak M., Crump, Alex R., Goldman, Amy E., Bramer, Lisa M., Evan, Arntzen C., Romero, Elvira, Resch, C. Tom, Kennedy, David W., Stegen, James C., 2017. Carbon inputs from riparian vegetation limit oxidation of physically bound organic carbon via biochemical and thermodynamic processes. J. Geophys. Res. Biogeosci. 122 (12), 3188–3205.
Grossman, J.N., Kahan, T.F., 2016. Hydroxyl radical formation from bacteria-assisted Fenton chemistry at neutral pH under environmentally relevant conditions. Environ. Chem. 13, 757. https://doi.org/10.1071/EN15256.
Guggenberger, Georg, Kaiser, Klaus, Zech, Wolfgang, 1998. Mobilization and immobilization of dissolved organic matter in forest soils. Z. Pflanzenern. Bodenk. 161 (4), 401–408.
Hall, S.J., Silver, W.L., 2013. Iron oxidation stimulates organic matter decomposition in humid tropical forest soils. Glob. Change Biol. 19 (9), 2804–2813. https://doi.org/10.1111/gcb.12229.
Hall, Steven J., Silver, Whendee L., Timokhin, Vitaliy I., Hammel, Kenneth E., 2015. Lignin decomposition is sustained under fluctuating redox conditions in humid tropical forest soils. Glob. Change Biol. 21 (7), 2818–2828.
Hall, Steven J., Silver, Whendee L., Timokhin, Vitaliy I., Hammel, Kenneth E., 2016. Iron addition to soil specifically stabilized lignin. Soil Biol. Biochem. 98 (July), 95–98.
Heim, A., Schmidt, M.W.I., 2007. Lignin turnover in arable soil and grassland analysed with two different labelling approaches. Eur. J. Soil Sci. 58 (3), 599–608.
Huang, Zaoquan, Lv, Jitao, Cao, Dong, Zhang, Shuzhen, 2019. Iron plays an important role in molecular fractionation of dissolved organic matter at soil-water interface. Sci. Total Environ. 670, 300–307.
Johnson, R.L., Schmidt-Rohr, K., 2014. Quantitative solid-state ^{13}C NMR with signal enhancement by multiple cross polarization. J. Magn. Reson. 239, 44–49. https://doi.org/10.1016/j.jmr.2013.11.009.
Kleber, Markus, Johnson, Mark G., 2010. Advances in understanding the molecular structure of soil organic matter. Adv. Agron. 106, 77–142.
Kleber, M., Eusterhues, K., Keiluweit, M., Mikutta, C., Mikutta, R., Nico, P.S., 2015. Mineral-organic associations: formation, properties, and relevance in soil environments, Adv. Agronomy. https://doi.org/10.1016/bs.agron.2014.10.005.
Kleber, Markus, Sollins, Phillip, Sutton, R., 2007. A conceptual model of organo-mineral interactions in soils: Self-assembly of organic molecular fragments into zonal structures on mineral surfaces. Biogeochemistry 85 (1), 9–24.
Klotzbücher, Thimo, Filley, Timothy R., Kaiser, Klaus, Kalbitz, Karsten, 2011. A study of lignin degradation in leaf and needle litter using 13C-labelled tetramethylammonium hydroxide (TMAH) thermochemolysis: Comparison with CuO oxidation and van Soest methods. Org. Geochem. 42 (10), 1271–1278.
Klotzbücher, Thimo, Kalbitz, Karsten, Cerli, Chiara, Hernes, Peter J., Kaiser, Klaus, 2016. Gone or just out of sight? The apparent disappearance of aromatic litter components in soils. SOIL 2 (3), 325–335.
Koch, B.P., Dittmar, T., 2016. From mass to structure: An aromaticity index for high-resolution mass data of natural organic matter. Rapid Commun. Mass Spectrom.: RCM 30 (1), 250.
Kok, Gregory L., 1980. Measurements of hydrogen peroxide in rainwater. Atmos. Environ. 14 (6), 653–656.
Kujawinski, Elizabeth B., Behn, Mark D., 2006. Automated analysis of electrospray ionization Fourier transform ion cyclotron resonance mass spectra of natural organic matter. Anal. Chem. 78 (13), 4363–4373.
LaRowe, Douglas E., Van Cappellen, Philippe, 2011. Degradation of natural organic matter: A thermodynamic analysis. Geochim. Cosmochim. Acta 75 (8), 2030–2042.
Lehmann, Johannes, Kleber, Markus, 2015. The contentious nature of soil organic matter. Nature November, 1–9.
Lv, Jitao, Zhang, Shuzhen, Wang, Songshan, Luo, Lei, Cao, Dong, Christie, Peter, 2016. Molecular-scale investigation with ESI-FT-ICR-MS on fractionation of dissolved organic matter induced by adsorption on iron oxyhydroxides. Environ. Sci. Technol. 50 (5), 2328–2336.
Mikutta, Robert, Mikutta, Christian, Kalbitz, Karsten, Scheel, Thorsten, Kaiser, Klaus, Jahn, Reinhold, 2007. Biodegradation of forest floor organic matter bound to minerals via different binding mechanisms. Geochim. Cosmochim. Acta 71 (10), 2569–2590.
Miller, C.J., Rose, A.L., Waite, T.D., 2016. Importance of iron complexation for Fenton-mediated hydroxyl radical production at circumneutral pH. Front. Mar. Sci. 3 https://doi.org/10.3389/fmars.2016.00134.
Moody, G.J., 1963. The action of Fenton's reagent on carbohydrates. Tetrahedron 19, 1705–1710. https://doi.org/10.1016/S0040-4020(01)99244-0.
Morelli, R., Russo-Volpe, S., Bruno, N., Lo Scalzo, R., 2003. Fenton-dependent damage to carbohydrates: Free radical scavenging activity of some simple sugars. J. Agric. Food Chem. 51, 7418–7425. https://doi.org/10.1021/jf030172q.
O'Donnell, Jonathan A., Aiken, George R., Butler, Kenna D., Guillemette, Francois, Podgorski, David C., Spencer, Robert G.M., 2016. DOM composition and transformation in boreal forest soils: The effects of temperature and organic-horizon decomposition state. J. Geophys. Res. Biogeosci. 121 (10), 2727–2744.
Ohno, Tsutomu, Parr, Thomas B., Gruselle, Marie-Cecile I., Fernandez, Ivan J., Sleighter, Rachel L., Hatcher, Patrick G., 2014. Molecular composition and biodegradability of soil organic matter: A case study comparing two new england forest types. Environ. Sci. Technol. 48, 7729–17236.
Ohno, Tsutomu, Sleighter, Rachel L., Hatcher, Patrick G., 2016. Comparative study of organic matter chemical characterization using negative and positive mode electrospray ionization ultrahigh-resolution mass spectrometry. Anal. Bioanal. Chem. 408 (10), 2497–2504.
Ohno, Tsutomu, Rachel L. Sleighter, Patrick G. Hatcher. 2018. Adsorptive Fractionation of Corn, Wheat, and Soybean Crop Residue Derived Water-Extractable Organic Matter on Iron (oxy)hydroxide. Geoderma 326 (November 2017): 156–63.
Page, S.E., Sander, M., Arnold, W.A., McNeill, K., 2012. Hydroxyl radical formation upon oxidation of reduced humic acids by oxygen in the dark. Environ. Sci. Technol. 46, 1590–1597. https://doi.org/10.1021/es203836f.
Patel, Kaizad F. 2020. kaizadp/fticrrr: FTICR-results-in-R (v0.1.0). https://github.com/kaizadp/fticrrr. DOI: 10.5281/zenodo.3893246.
Patel, Kaizad F., Fernandez, Ivan J., Nelson, Sarah J., Gruselle, Marie-Cécile, Norton, Stephen A., Weiskittel, Aaron R., 2019. Forest N dynamics after 25 years of whole watershed n enrichment: The Bear Brook Watershed in Maine. Soil Sci. Soc. Am. J. Soil Sci. Soc. Am. 83 (s1), S161.
Petigara, Bhakti R., Blough, Neil V., Mignerey, Alice C., 2002. Mechanisms of hydrogen peroxide decomposition in soils. Environ. Sci. Technol. 36 (4), 639–645.
Prein, Andreas F., Rasmussen, Roy M., Ikeda, Kyoko, Liu, Changhai, Clark, Martyn P., Holland, Greg J., 2017. The future intensification of hourly precipitation extremes. Nat. Clim. Change 7 (1), 48–52.
Riedel, T., Biester, H., Dittmar, T., 2012. Molecular fractionation of dissolved organic matter with metal salts. Environ. Sci. Technol. 46 (8), 4419–4426. https://doi.org/10.1021/es203901u.
Schmidt, Michael W.I., Torn, Margaret S., Abiven, Samuel, Guggenberger, Thorsten Dittmar Georg, Janssens, Ivan A., Kleber, Markus, et al., 2011. Persistence of soil organic matter as an ecosystem property. Nature 478 (7367), 49–56.
Schneider, M.P.W., Scheel, T., Mikutta, R., van Hees, P., Kaiser, K., Kalbitz, K., 2010. Sorptive stabilization of organic matter by amorphous Al hydroxide. Geochim. Cosmochim. Acta 74 (5), 1606–1619.
Seidel, Michael, Beck, Melanie, Riedel, Thomas, Waska, Hannelore, Suryaputra, I.G.N.A., Schnetger, Bernhard, Niggemann, Jutta, Simon, Meinhard, Dittmar, Thorsten, 2014. Biogeochemistry of dissolved organic matter in an anoxic intertidal creek bank. Geochim. Cosmochim. Acta 140 (September), 418–434.
Simon, Carsten, Vanessa-Nina Roth, Thorsten Dittmar, and Gerd Gleixner. 2018. Molecular signals of heterogeneous terrestrial environments identified in dissolved organic matter: a comparative analysis of orbitrap and ion cyclotron resonance mass spectrometers. Front. Earth Sci. China 6 (September). https://doi.org/10.3389/feart.2018.00138.
Thieme, Lisa, Daniel Graeber, Diana Hofmann, Sebastian Bischoff, Martin T. Schwarz, Bernhard Steffen, Ulf-Niklas Meyer, et al. 2019. "Dissolved Organic Matter Characteristics of Deciduous and Coniferous Forests with Variable Management: Different at the Source, Aligned in the Soil.".
Sleighter, Rachel L., McKee, Georgina A., Liu, Zhanfei, Hatcher, Patrick G., 2008. Naturally present fatty acids as internal calibrants for Fourier transform mass spectra of dissolved organic matter. Limnol. Oceanogr. Methods 6, 246–253. https://doi.org/10.4319/lom.2008.6.246.
Tolić, Nikola, Liu, Yina, Liyu, Andrey, Shen, Yufeng, Tfaily, Malak M., Kujawinski, Elizabeth B., Longnecker, Krista, et al., 2017. Formularity: Software for automated formula assignment of natural and other organic matter from ultrahigh-resolution mass spectra. Anal. Chem. 89 (23), 12659–12665.
Trusiak, Adrianna, Treibergs, Lija A., Kling, George W., Cory, Rose M., 2018. The role of iron and reactive oxygen species in the production of CO_2 in Arctic soil waters. Geochim. Cosmochim. Acta 224 (March), 80–95.
Waggoner, Derek C., Chen, Hongmei, Willoughby, Amanda S., Hatcher, Patrick G., 2015. Formation of black carbon-like and alicyclic aliphatic compounds by hydroxyl radical initiated degradation of lignin. Org Geochem. 82 (May), 69–76.
Waggoner, Derek C., Wozniak, Andrew S., Cory, Rose M., Hatcher, Patrick G., 2017. The role of reactive oxygen species in the degradation of lignin derived dissolved organic matter. Geochim. Cosmochim. Acta 208 (July), 171–184.
Yang, Wendy H., Liptzin, Daniel, 2015. High potential for iron reduction in upland soils. Ecology 96 (7), 2015–2020.
Young, Robert, Avneri-Katz, Shani, McKenna, Amy, Chen, Huan, Bahureksa, William, Polubesova, Tamara, Chefetz, Benny, Borch, Thomas, 2018. Composition-dependent sorptive fractionation of anthropogenic dissolved organic matter by Fe(III)-montmorillonite. Soil Syst. 2 (1), 14.